Colloid and Polymer Science (2023) 301:75–92
https://doi.org/10.1007/s00396-022-05039-0

ORIGINAL CONTRIBUTION

Thermoresponsive phase behavior and nanoscale self-assembly generation in normal and reverse Pluronics®

Dhruvi Patel[1] · Payal Vaswani[2] · Sumana Sengupta[3,4] · Debes Ray[5] · Dhiraj Bhatia[2] · Sharmistha Dutta Choudhury[3,4] · Vinod K. Aswal[5] · Ketan Kuperkar[1] · Pratap Bahadur[6]

Received: 26 September 2022 / Revised: 19 October 2022 / Accepted: 20 October 2022 / Published online: 7 December 2022

Abstract

Self-assembly generation in block copolymers (BCPs): normal Pluronics® (L31, L64, L35, P65) and reverse Pluronics® (31R1, 17R4, 25R4, 10R5) are scrutinized in single/ mixed aqueous environment systems. Solutions up to 10%w/v in investigated systems remained transparent up to ambient temperature while on progressive heating they attained their cloud point (CP). The critical micelle temperature (CMT) was evaluated by fluorescence spectroscopy, which is further complemented by dynamic light scattering (DLS) and small-angle light scattering (SANS). L31 showed phase separation (2ϕ) at ~ 30 °C without any micelle formation. L64, L35, and P65 formed micelles at high temperatures with some growth close to CP while all reverse Pluronics® formed no micelles until CP. The micellar parameters were reinforced from scattering as a function of temperature. Furthermore, these nanoscale micellar aggregates were explored qualitatively and quantitatively as potential nanocargos for anticancer (curcumin) drug to understand the cytotoxic effect using MTT assay.

Keywords Block copolymers (BCPs) · Phase behavior · Micellar transition · Scattering profile · Drug solubilization

Introduction

Block copolymers (BCPs) architect as interchanging blocks of ethylene oxide (EO) and propylene oxide (PO) have reflected a renowned fascination in the field of research since several decades. The linear BCPs are commercially accessible as normal (EO-PO-EO) and reverse (PO-EO-PO) Pluronics®. These BCPs offer a diverse and intricate self-aggregation in solution environment due to the varying composition of PO molecular weight, % EO, and wide range of hydrophilic-lipophilic balance (HLB) [1–4]. Water is considered as a selective solvent for these BCPs, i.e., a decent solvent for EO blocks and comparatively poor solvent for the PO blocks. Studies have extensively reported the self-assembly of these amphiphilic BCPs because of their thermoresponsive, biocompatible, and non-toxic response which enable them to serve as effective drug delivery vehicle. Some of them are granted by the Food and Drug Administration (FDA) and practiced often in personal care formulations, food additives, etc. [5–8]. Studies have also explored the phase diagram, micellar behavior and reversible thermo-rheological features of normal Pluronics® in aqueous solution [9–11]. Usually, these amphiphilic entities under applied stimuli exhibit varied nanoscale assemblies such as unimers or Gaussian chain or micelles and often show shape transition leading progressively to phase separation (2ϕ), i.e., cloud point (CP) [12].

The amalgamated interest for Pluronics® has led the scientists to unfold the novel kind of BCPs with similar structure which demonstrate interesting micellization or aggregation behavior that can offer a wide range of solution

✉ Ketan Kuperkar
ketankuperkar@gmail.com

1 Department of Chemistry, Sardar Vallabhbhai National Institute of Technology (SVNIT), Ichchhanath, Surat 395 007, Gujarat, India

2 Biomedical Engineering, Indian Institute of Technology Gandhinagar (IITGn), Palaj, Gandhinagar 382 355, Gujarat, India

3 Radiation and Photochemistry Division, Bhabha Atomic Research Centre (BARC), Mumbai-400 085, Trombay, Maharashtra, India

4 Homi Bhabha National Institute, Anushaktinagar, Mumbai 400 094, India

5 Solid State Physics Division, Bhabha Atomic Research Centre (BARC), Trombay, Mumbai 400 085, Maharashtra, India

6 Department of Chemistry, Veer Narmad South Gujarat University (VNSGU), Surat 395007, Gujarat, India

properties unified with applications as a function of stimuli. Lin and Paschalis. investigated the temperature effect on aggregation behavior of L64 using neutron scattering [13]. Tsui et al. explored the micellization behavior of F68 and F88 in aqueous solution using calorimetry and found that the CMT increases with the decrease in BCP concentration [14]. Ganguly et al. showed the influence of SDS on the self-assembly of P85, P123, and F127 along with the micellar gel phase [15]. Patel et al. examined the salt-triggered self-assembly in F88 and illustrated the micellar transition with the addition of inorganic salt [16]. Alvarez-Ramirez et al. reported the phase behavior and the rheological response of P103 in the dilute and semi-dilute regimes [17]. Basak and Bandyopadhyay . scrutinized the temperature and pH effect on the spherical micelles of F127 which were used for hydrophobic drug encapsulation [18]. Popovici et al. described the antimicrobial activity of active pharmaceutical ingredient, 1-(5′-nitrobenzimidazole-2′-yl-sulphonyl-acetyl)-4-aryl-thiosemicarbazide in F127 micelles [19]. Mata et al. reported the self-assembly of L64 as a function of concentration and temperature in water [20]. Also, a number of studies have demonstrated the micellization phenomenon in normal Pluronics® in presence of additives like salts, alcohols, amines, acids, and surfactants [21–23].

Like normal Pluronics®, reverse Pluronics® show a contrast influence on the CP of BCPs in aqueous solution [24]. Few authors have stated experimental evidences for reverse BCPs undergoing micellization in dilute aqueous solution. Those with low PEO (highly hydrophobic) undergo 2ϕ below ambient temperature (CP < 20 °C) in compare to their normal counterparts. However, for moderately hydrophobic BCPs, the micellization window is very small and often forms micelle or loose aggregates close to their CP. In spite of their enormous use in various fields, literature on reverse BCPs is deficient when compared to normal BCPs, in terms of their associative properties, specifically in dilute solution. Kumi et al. reported the self-association of the reverse Pluronic® 17R4 in deuterium oxide (D_2O) where it exists as unimers at the lowest temperature and mass fractions. The formation of flower micelles by 17R4 was noted with insoluble end blocks. [25]. Chowdhry et al. described the phase transitions in 31R1 by calorimetric investigation [26]. D'Errico et al. demonstrated the temperature and concentration effect on the aggregation and phase behavior for 25R4 [8]. Guiraud et al. promoted 25R2 for DNA transfection of skeletal muscle in a similar manner as P105 [27].

Supramolecular aggregates like micelles, vesicles, liposomes, and lyotropic liquid crystalline phases from BCPs are established as suitable candidates as drug carriers [28–30]. Very promisingly, these BCPs micelles are estimated in several clinical trials as fine transporters for anticancer drugs due to their small particle size (< 100 nm), brilliant targeting ability, and long circulation. Here, the hydrophobic micellar core serves as a reservoir for the encapsulation of lipophilic drug, while the hydrophilic corona stabilizes the hydrophobic core.

In addition to the single micellar system, the BCPs in mixed micellar environment have also been documented as nanocargos for designing a better drug delivery system which can be widely used for high drug loading and good release profile for enhanced bioavailability without any toxicological consequences [31–38]. However, such aggregate formation depends on the BCP molecular structure, temperature, solvent, concentration, mixing ratio, etc. A lot of literature exist on mixed systems comprising of different Pluronics® in drug delivery systems. Zhang et al. reported P123 and F127 mixed system for the treatment of multidrug resistant tumors [35]. Dutra et al. described the F127 and P123 mixed micelles for griseofulvin solubilization [28]. El-Dahmy et al. aimed to increase the in vivo mean residence time of drug using mixed micellar systems from L121, P123, and F127 [29]. Zhao et al. prepared and optimized the curcumin-loaded mixed micelles of P123 and F68 [30]. Hassanzadeh et al. synthesized F127 and 10R5 mixed micelles for doxorubicin to enhance its therapeutic function and reducing the side effects to normal cells [37].

Very particularly, studies have presented the use of various drug carriers such as cyclodextrins, proteins, peptides, dendrimers, polymers for curcumin encapsulation. Camelia-Elena et al. examined the influence of the curcumin loading on the pH-sensitive poly(2-vinyl pyridine)-b-poly(ethylene oxide) ($P2VP_{90}$-b-PEO_{398}) micelles [39]. The same group also reported curcumin-loaded polysaccharides-based complex particles obtained by polyelectrolyte complexation and ionic gelation [40, 41]. Jingliang et al. reported the liposomes-based curcumin delivery [42]. Vivek et al. testified the effect of cyclodextrin complexation of curcumin on its solubility and antiangiogenic and anti-inflammatory activity in rat colitis model [43]. Patel et al. reported the curcumin solubilization and release profile for polymeric micelles [38, 44].

However, to the best of our knowledge, studies on normal and reverse mixed Pluronics® in curcumin encapsulation is still unexplored. Differently from the various literatures, here the similar structure of BCPs with different block arrangement both in single and mix environment has not been investigated in detail. Thus, the present work aims to examine the phase behavior and micellar growth/transition in aqueous mixture solution of normal and reverse BCPs. A keen observation on the phase behavior of these solutions has been given an account to identify the concentration and temperature effect on micellization. Solution behavior with the temperature aging change the solution appearance and proposed varied micellar growth/transition and finally leading to 2ϕ. Furthermore, the probable geometries or cloudiness of the solution has been revealed from the dynamic

Scheme 1 Structural constitution and molecular characteristics of the examined BCPs

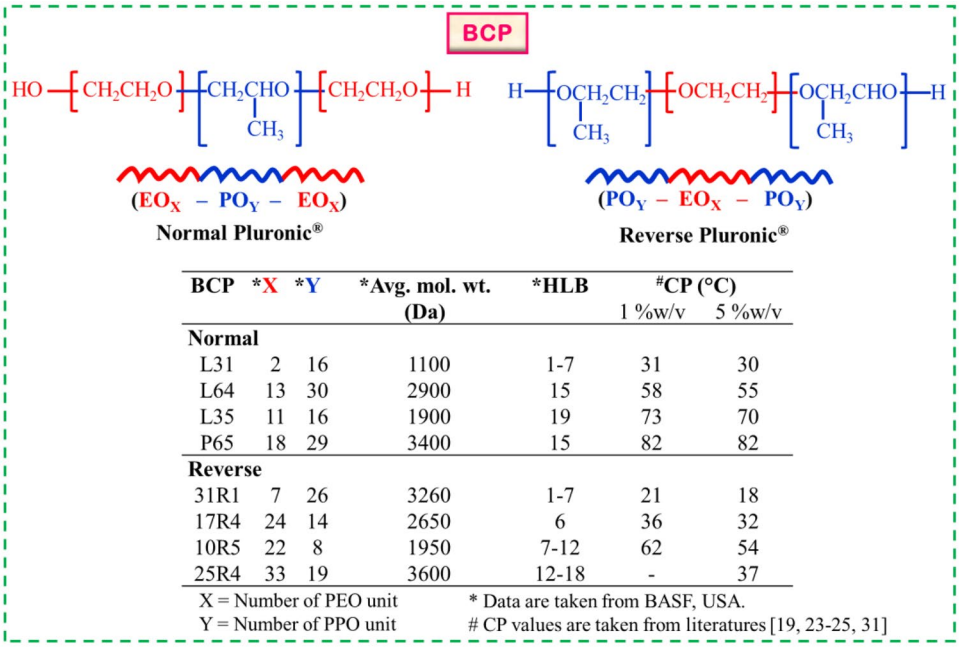

BCP	*X	*Y	*Avg. mol. wt. (Da)	*HLB	#CP (°C) 1 %w/v	5 %w/v
Normal						
L31	2	16	1100	1-7	31	30
L64	13	30	2900	15	58	55
L35	11	16	1900	19	73	70
P65	18	29	3400	15	82	82
Reverse						
31R1	7	26	3260	1-7	21	18
17R4	24	14	2650	6	36	32
10R5	22	8	1950	7-12	62	54
25R4	33	19	3600	12-18	-	37

X = Number of PEO unit
Y = Number of PPO unit
* Data are taken from BASF, USA.
# CP values are taken from literatures [19, 23-25, 31]

light scattering (DLS) technique that scrutinize the micellar size (D_h) of normal BCPs, reverse BCPs, and their mixtures in varying % weight fraction as function of temperature. In addition, the probable micellar shapes and aggregation will be predicted from the small-angle neutron scattering (SANS). This nanoscale self-assembly generation in normal and reverse single and mixed micelles will be put on the quantitative and qualitative check for the solubilization of anticancer drug curcumin (Cur) using UV–Vis spectroscopy. For the practical implementation of our examined system, a cytotoxicity study was undertaken to explore the nanocargos as potential candidate in drug delivery system.

Experimental section

Materials

EO-PO-based (normal) and PO-EO-based (reverse) triblock copolymers (BCP) made available as gift samples from BASF, NJ, USA. The structures and molecular characteristics of the used BCPs are presented in Scheme 1. The anticancer drug, curcumin (Cur), was purchased from SD Fine, BRL, IN. All the acquired chemicals ingredients were used as such without any further purification.

For the neutron scattering experiments, the sample solutions were prepared in deuterium oxide (D_2O) to obtain a good contrast between the hydrophobic core and the solvent while for the rest of the studies, the solutions were prepared in double-distilled water. Before each measurement, the sample solutions were filtered using a nylon filter having pore diameter of ~ 0.45 µm.

Methods

Phase behavior

BCP solutions within the range 1 to 10%w/v were prepared using double-distilled water. The cloud point (CP) was observed by gentle heating (rate of heating ~ 0.1 °C) of the prepared solutions in a glass vial (2 mL) with constant stirring up to 90 °C until its texture appears either clear/bluish or cloudy. The error in their CP measurements was within the range ± 0.2 °C [32–34].

Fluorescence spectroscopy

The critical micelle temperature (CMT) of 10%w/v micellar solutions composed of varying ratios of BCPs was determined using monomeric pyrene as the fluorescent probe. Fluorescence spectra were recorded within the spectral range of 350–500 nm on a Shimadzu spectrofluorometer (RF-6000) with an excitation wavelength of 335 nm. The temperature of the sample chamber was controlled by a circulating water bath. The intensity ratio of the first and third vibrational bands in the fluorescence spectra of pyrene (I_1/I_3) was plotted as a function of temperature. The inflection point in the curve was considered as a direct indication of micelle formation and was noted as the CMT [35–38].

Light scattering

Dynamic light scattering (DLS) experiments were performed for 10%w/v BCP solutions with temperature scan on Malvern instrument, UK to obtain the hydrodynamic diameter (D_h). Before every measurement, the scattering cells were drowned in acetone and dried immediately before use. DLS uses argon laser as the incident beam where the scattering was achieved using vertically polarized light having wavelength ~ 514.5 nm and scattering angle 90°.The experiments were repeated five times to check the reproducibility. [30, 31].

Neutron scattering

Small-angle neutron scattering (SANS) experiments were performed at Dhruva reactor, BARC, India. The coherent differential scattering cross-section ($d\Sigma/d\Omega$) per unit volume as a function of wave vector transfer Q is measured. Here, the mean wavelength of the monochromatized beam is 5.2 Å with a spread of $\Delta\lambda/\lambda \sim 15\%$. The instrument covers a Q range of 0.017–0.35 $Å^{-1}$ with sample slit size: 1.3 cm and source slit size: 5 cm × 3 cm. The scattering data were corrected for the background and the empty cell contributions were subsequently normalized to the absolute cross-sectional unit using the standard protocols. Here, the obtained data were fitted using SASFIT program [16, 34–36].

Drug solubilization

The absorption spectra were studied using Model-Cary 50 Varian to confirm the solubilization proficiency of curcumin (Cur) ($\lambda_{max} = \sim 425$ nm) in the 10%w/v mixed micelles of normal and reverse Pluronics® environment. The drug-loaded micellar system were prepared by adding an excess amount of the Cur into the mixed micellar solutions and agitated at 30 °C for 2–3 days. These solutions were further filtered using ~ 0.45 µm filter to remove the undissolved Cur and diluted with ethanol about ~ 10 times to obtain the absorbance spectra in range of ~ 200 to 800 nm [34–36].

Cell culture

HeLa cells (cervical cancer) were cultured and maintained in Dulbecco's modified Eagle medium (DMEM, Lonza) supplemented with 10% (v/v) fetal bovine serum (FBS, Gibco, USA) and 1% (v/v) Penstrep solution (Himedia, India) in a humidified incubator at 37 °C with 5% CO_2 [37–42].

In vitro *cytotoxicity assay*

The cytotoxicity of all the compounds were assessed using MTT assay (3-(4, 5-dimethylthiazol-2-yl)-2, 5-diphenyl tetrasodium bromide, Thermo Fischer Scientific) against the HeLa cell line. The compounds were tested at varying concentration ranges from 100 to 1000 ng/mL. All cells were trypsinized and seeded into a 96-well plate for the assay and allowed to adhere for 24 h. At their 85–90% confluency, the cells were incubated for 4 h with the concentration gradient (100, 200, 400, 600, 800, and 1000 ng/mL) of the compounds with DMEM serum-free media. The media was then decanted and the cells were treated with 100 µL of MTT (5 ng/mL stock) prepared in PBS and incubated for 4 h. The formed formazan crystals were solubilized in 100 µL DMSO and absorbance was taken at 570 nm using a Multiplate reader (Bioteck). The percentage viability was calculated by normalizing the absorbance value of the test sample with untreated control. The curve was plotted for concentration versus normalized cell viability. The IC_{50} value was determined for each compound [43–47].

Cellular uptake

The HeLa cells were trypsinized and seeded in 12-well plates on coverslips. After attaining 80–90% confluency, the cells were treated with all the compounds at 1 µg/mL in DMEM serum-free media and incubated for 1 h at 37 °C. The media was decanted and washed (2 ×) gently by PBS. The cells were further fixed using 4% paraformaldehyde (PFA) solution at 37 °C for 15 min. The cells were washed with PBS (3 ×) to remove any residual PFA. The coverslips were then mounted on slides using Mowiol. The bright field images were captured under a fluorescence microscope (Nikon) at 10 × magnification and are further processed using ImageJ software [45–47].

Results and discussion

Phase behavior

Pluronics® solution exhibit lower critical solution temperature (LCST) between 15 and > 100 °C and show opulent phase behavior by increasing the solution concentration comprising reversible thermo-rheological gelation [6, 16]. The PEO and PPO blocks being miscible in water make the copolymer molecularly dissolved and form either unimers or Gaussian coil below the critical micellization temperature (CMT). However, the solubility of the PPO blocks gradually decreases as the temperature ages to CMT, succeeding the onset of micellization. Progressively, the PEO blocks experience dehydration by temperature aging and further the solution undergoes phase separation (2ϕ), i.e., cloud point (CP). Reports on the clouding behavior of normal Pluronics® are available [19–22, 28–31] while literature reporting the clouding demeanor of reverse Pluronics® is very limited [24–26].

Among all the Pluronics® tested, normal Pluronic® L31 (having 10% PEO content and low molecular weight) exhibit CP between ~ 40 and ~ 28 °C as its concentration increase from 1 to 10%w/v respectively. While it is reverse counterpart 31R1 has CP values between ~ 26 and ~ 20 °C from 1 to 10%w/v respectively (Fig. 1a). Such CP trend displayed by hydrophobic Pluronics® (L31 and 31R1) infers the probable presence of unimers along with the loose clusters close to their CP. Such behavior goes well in agreement with the reported low molecular weight PPO and highly water insoluble homopolymers. Similarly, moderate hydrophilic Pluronics® (40% PEO), i.e., L64 show the CP values between ~ 73 and ~ 63 °C from 1 to 10%w/v respectively, whereas its reverse analog, i.e., 17R4 display the CP between ~ 49 and ~ 39 °C from 1 to 10%w/v solution respectively (Fig. 1a). Such behavior attribute L64 to form micelles above CMT which grow in size at temperature close to CP but 17R4 remain as unimers with loose clusters up to CP. A like behavior was noted in case of partial hydrophilic Pluronics® (50% PEO) where L35 revealed the clouding behavior ranging between ~ 87 and ~ 73 °C and ranging between ~ 74 to ~ 58 °C from 1 to 10%w/v for 10R5, respectively (Fig. 1a). Both these BCPs remain as unimers until a wide temperature range due to 50% PEO and behave like PEO homopolymers (highly water soluble and unable to self-assembled). Furthermore, L35 at higher temperature displays micellar growth near to its CP whereas 10R5 remain as unimers throughout its CP. The CP of P65 (50% PEO) and 25R4 (40% PEO) having similar molecular weight are also examined. Here, P65 behaves similar like L35 with its CP from ~ 86 to ~ 81 °C, whereas the reverse entity 25R4 show similar behavior like 17R4 with its CP between ~ 48 and ~ 37 °C respectively from 1 to 10%w/v (Fig. 1a).

In our case, the CP of normal BCPs is seen to decline linearly with increase in its concentration. Such a decrease in CP indicates the plausible micellar shape transition from unimers to hydrated globular coil to either spherical core–shell micelles or even to higher order of geometry. In the non-polar cavity of reverse BCP, the penetration of PEO segment is not possible due to steric hindrance and polarity restrictions. As a result, the species produce clusters with an increase in concentration that makes the CP to continuously decline.

There is no CP literature reported showing the aqueous solution behavior of normal and reverse Pluronics® in mixtures with their perfect pairing giving an account to % PEO and mol. wt. in various ratios (% weight fraction). Figure 1b illustrates the clouding behavior of normal and reverse Pluronics® in mixed compositions where it was observed that the mixtures behave much differently from their individual counterparts thereby anticipating favorable interactions between the two copolymeric sequences. With this rationale, for mixed micellar BCP systems, 10%w/v normal and reverse BCP were mixed in varying % weight fraction ratio (1:0, 0.75:0.25, 0.5:0.5, 0.25:0.75, and 0:1). L31 and 31R1 when mixed in varying ratio showed the CP between ~ 28 and ~ 20 °C, while the mixture for L64:17R4, L35:10R5, and P65:25R4 displayed the CP between ~ 63 and ~ 39 °C, ~ 73 to ~ 58 °C, and in range of ~ 81 to ~ 37 °C, respectively. Such trend inferred that CP of normal BCPs decrease by the addition of reverse BCP. However, only single CP was observed for all examined systems which depict proper homogenous mixing of both the BCPs in aqueous solution. Thus, we can deliberate that normal and reverse BCPs have their unique individualities in the solution with respect to their superlative clouding phenomenon.

Micellization conduct

Reported literatures have shown the self-assembly determination and critical micellization temperature (CMT) measurements of varied BCPs in single and mixed environment performed by fluorescence spectroscopy [16, 28]. The purpose of selecting pyrene as fluorescent probe is that it being extremely hydrophobic, favorably migrates into the PPO (hydrophobic) microdomains in an aqueous solution and show strong fluorescence in non-polar environment, whereas weak fluorescence intensity in a polar environment

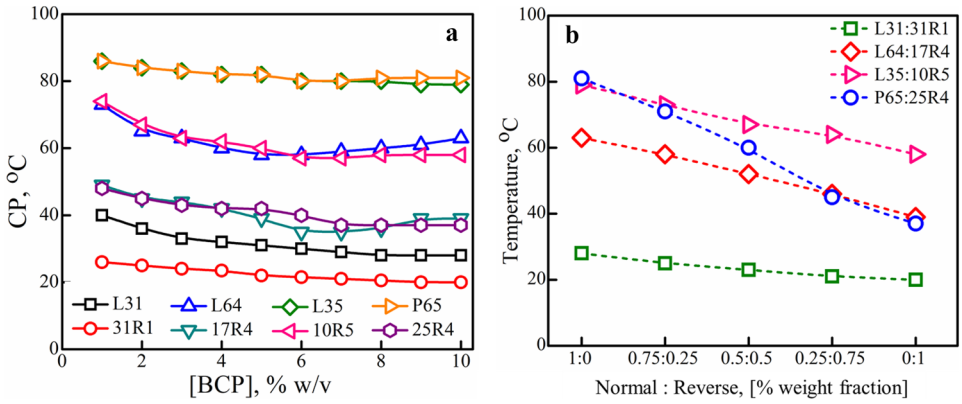

Fig. 1 Clouding demeanor of 10%w/v normal and reverse triblock copolymers (BCPs) as function of concentration (% w/v) for **a** single system and **b** mixed system

causes the shifting in I_1/I_3 ratio in the emission peak [24, 29]. Figure 2 presents the pyrene dependence fluorescence intensity ratio (I_1/I_3) as a function of temperature in different BCPs and their mixtures.

Since the normal Pluronic® L31 undergoes 2ϕ at ~ 28 °C while its reverse counterpart 31R1 has CP at ~ 20 °C, CMT measurements for the L31:31R1 system could not be carried out within the studied temperature range (20 to 60 °C). For the 10%w/v L64:17R4 system, the plots of I_1/I_3 versus temperature display a clear shift in their inflection towards higher temperatures, with increasing concentrations of 17R4 (Fig. 2a). Thus, for L64 alone, the CMT is found to be ~ 26 °C, while for L64:17R4 mixtures with ratios of 0.75:0.25, 0.5:0.5, 0.25:0.75, and 0:1, the corresponding CMT values are ~ 27 °C, ~ 29 °C, ~ 33 °C, and ~ 41 °C, respectively. This is clear indications that while the L64:17R4 system forms mixed micelles at all compositions; addition of 17R4 in L64 delays the micellization. In 10%w/v L35:10R5, the I_1/I_3 versus temperature plots of pyrene do not display inflections at any of the three investigated ratios (Fig. 2b), which suggests that these two components are unable to form micelles even in mixed scheme. For 10%w/v P65:25R4 system, the CMT values were ~ 32 °C and ~ 29 °C for 1:0 and 0.5:0.5, respectively. On the other hand, the reverse Pluronics® by itself, i.e., at 0:1 composition, do not undergo any micelle formation as indicated by the absence of any inflection in the I_1/I_3 versus temperature plot (Fig. 2c). Such behavior in the intensity profile goes well with the reported literature that presents the electrostatically held pyrene-mixed Pluronic® micelles that facilitate the migration of pyrene towards micellar core region and render more hydrophobicity which may cause plausible morphology transition with temperature [27–29]. Such shape change is further explored from the scattering studies.

Scattering profile

Reported studies have inferred that PEO backbone break the ether-water hydrogen bond that results into structural transition under the influence of temperature [24, 25, 35–37]. Also, it is well understood that the PPO blocks show dehydration than PEO blocks during the micellization process. Thus, the arrangement of such constitutional blocks in BCPs holds a major impact on the solution properties of BCPs. For our study, the confirmation of varied supramolecular micellar structures like unimers, Gaussian coil, core–shell micelles (spherical, ellipsoidal, flower-like), or network-like structures formed by BCPs in aqueous solution regime were scrutinized by scattering approach to establish the influence of temperature (Figs. 3, 4, and 5). It was noticed that the temperature influences the 2ϕ of BCPs profoundly which was quantified with respect to temperature aging and varying weight fractions (1:0, 0.75:0.25, 0.5:0.5, 0.25:0.75, and 0:1) of normal and reverse BCPs in single and mix solution

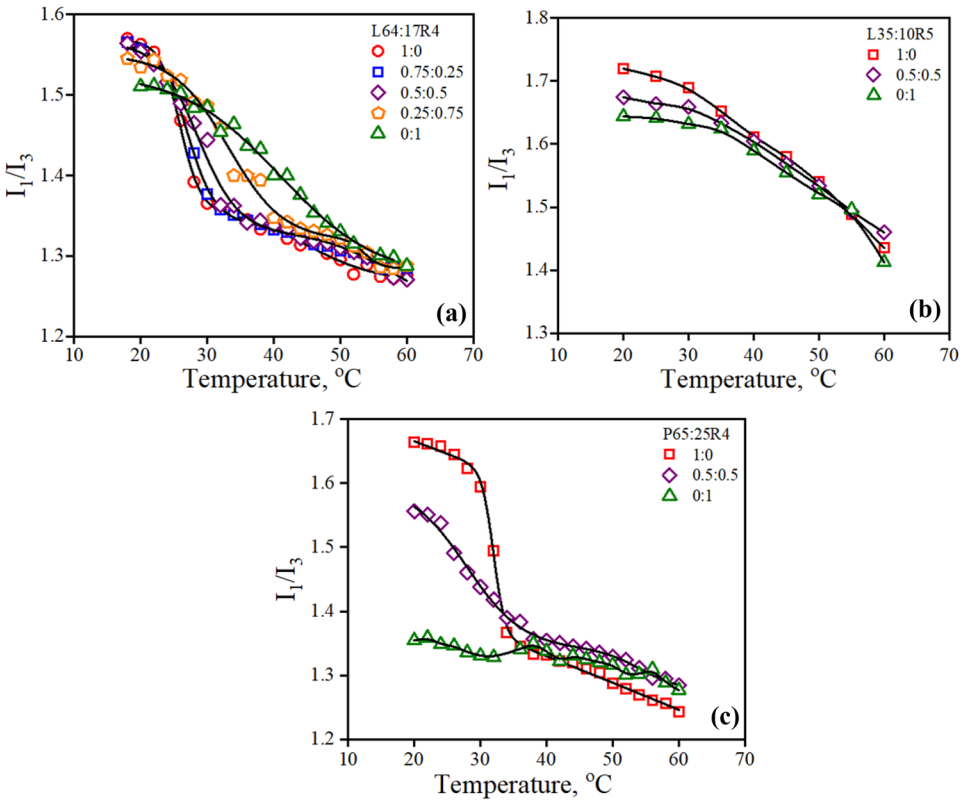

Fig. 2 CMT as determined by the variation in I1/I3 of pyrene emission with temperature for 10%w/v BCP in varying mix ratio for **a** L64:17R4, **b** L35:10R5, and **c** P65:25R4

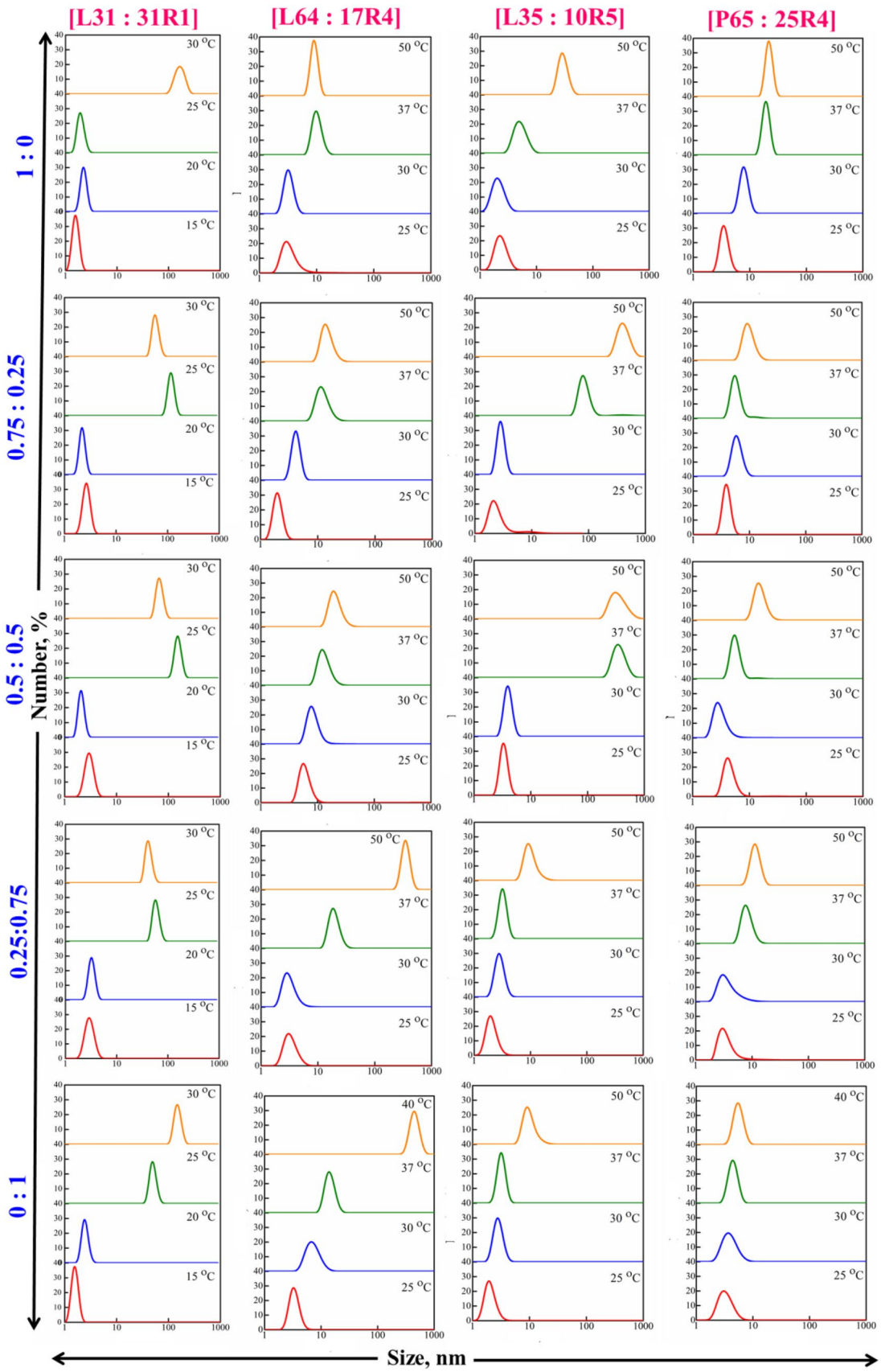

Fig. 3 Hydrodynamic size (Dh) distribution profile of 10%w/v BCP in varied weight fraction (single and mixed) combination with temperature aging

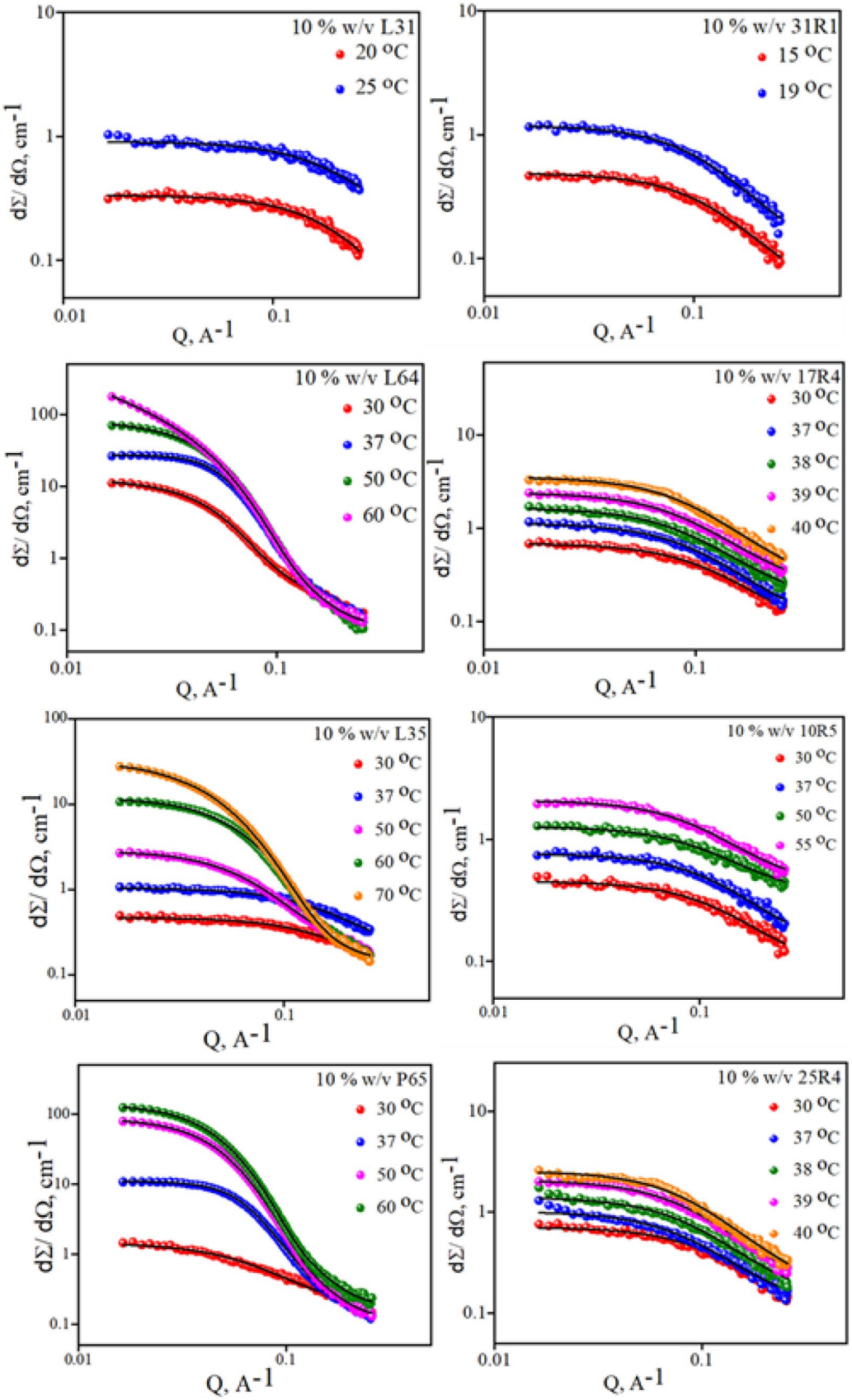

Fig. 4 Fitted scattering profile for 10%w/v BCP in aqueous medium as function of temperature

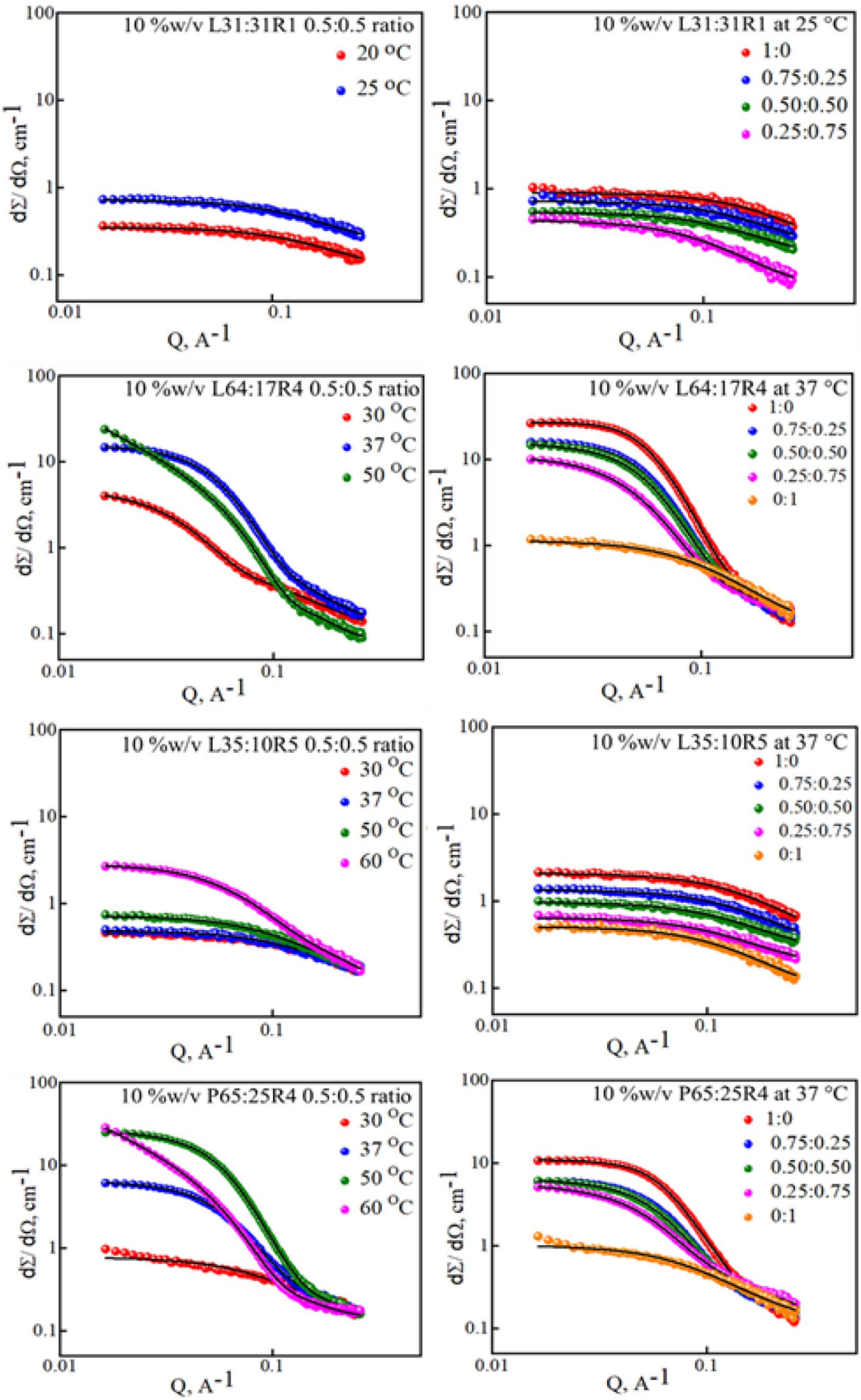

Fig. 5 Fitted scattering profile for 10%w/v BCP in mixtures of varying ratio as function of temperature

environment. Upon increasing the temperature in the threshold CMT region, the average hydrodynamic diameter (D_h) increases to form micelle/ clusters.

The cloudiness in 10% w/v L31 and 31R1 as individual owe to the larger knots of PPO blocks than the individual PEO. The D_h of 10%w/v L31 show single peak between ~ 2 and ~ 6 nm from temperature 15 to 25 °C respectively, thereby resembling the presence of unimers which turns into large clusters of several hundreds of nm at 30 °C. Such behavior attribute to the knotting and globular arrangements of the constitutional blocks that progressively lead to 2ϕ. While the reverse counterpart, i.e., 10%w/v 31R1 demonstrates the D_h between ~ 3 and ~ 6 nm from 15 and 20 °C respectively, later precipitate out above 25 °C, thereby showing large $D_h > 1000$ nm. The D_h results for their mixture (10%w/v L31:31R1) in varying % weight fraction ratio (0.75:0.25, 0.5:0.5, 0.25:0.75) displayed unimers around ~ 5 nm to larger cluster > 1000 nm from 15 to 30 °C which inferred that size of mixed Pluronics® appear larger than their individual counterparts (Fig. 3).

Similarly, the D_h profile for 10%w/v L64 show unimers around ~ 8 nm until 30 °C which grow around ~ 20 nm at 37 °C depicting the presence of spherical micelles that further grow up to ~ 50 nm at 50 °C. The clouding activities of 17R4 in water and its tendency to undergo self-assembly dramatically differ from L64. The 10%w/v reverse counterpart (17R4) show single peak of unimers around ~ 5 nm at 25 °C with a little increase in D_h, thereby representing unimers of around ~ 10 nm at 30 °C that turns probably into much large globular chains or flower-like reverse micelle of ~ 20 nm at 37 °C and progressively leading to the large clusters of the size > 1000 nm at 40 °C due to CP. Thus, L64 show an obvious micellar growth while 17R4 form unimers or small-scale micelles in water. However, for 10%w/v L64:17R4 mixed system, the 0.75:0.25 showed the unimers to gradual micelle formation from 25 to 50 °C due to higher content of L64 dominating its behavior on 17R4, while 0.5:0.5 ratio demonstrate the presence of unimers and micellar growth from 25 to 50 °C but the D_h gets affected by equal contribution of L64 and 17R4 in mixed micellization. For 0.25:0.75 ratio, it seems to behave like 17R4. Here, it shows the unimers to high-order micelles until 50 °C as water gets exorcized from the hydrophobic PPO core leading to CP (Fig. 3).

The 10%w/v L35 show unimers of ~ 5 nm at 25 °C, ~ 7 nm at 30 °C, ~ 10 nm at 37 °C, and probably spherical micelle ~ 30 nm at 50 °C while its counterpart 10%w/v 10R5 remain as unimers of about ~ 4 to ~ 15 nm throughout the temperature range of 25 to 50 °C. This may be due to its loose packing. However, the mixed micelles of 10%w/v L35:10R5 in varying weight fraction ratio showed interesting behavior. The 0.75:0.25 and 0.5:0.5 suggest the unimers to spherical micelle from 25 to 50 °C. For 0.25:0.75, the mixture remained as unimers throughout the temperature range (25 to 50 °C) due to higher impact of 10R5 on L35 (Fig. 3).

The D_h profile of 10%w/v P65 and 25R4 was also examined due to similar molecular weight and irrespective to their equal %PEO contribution (Fig. 3). P65 showed the presence of unimers until 30 °C while it associates to spherical micelles from 37 °C. 25R4 remained as unimers until 37 °C and showed $D_h > 1000$ nm at 50 °C depicting the presence of large clusters due to 2ϕ. 25R4 at lower temperature depict the presence of unimers dispersed in solution and form clusters at higher temperature. 10%w/v P65:25R4 mixed system show an interesting behavior. For 0.75:0.25 ratio, it remains as unimers untill 37 °C and form spherical micelle (~ 15 nm) at 50 °C. Similar observations were noted for 0.5:0.5 ratio due to equal impact on micellization while for 0.25:0.75 ratio, unimers (~ 6 nm) were observed until 30 °C and spherical micelle formation from 37 °C onwards. Thus, in strong contrast to normal copolymers, the reverse copolymeric unimers cover the wide range of concentration and temperature. An increase in weight fraction of normal Pluronic® to reverse analogues in single and mixed environment causes a shift in the micellar peaks which infer that the micelle exists at lower weight fraction of reverse BCPs while at its higher concentration, large amount of clusters is found in equilibrium with micelles of normal Pluronic®. Thus, the micellar species formed from reverse BCPs are more soluble and undergo poor assembly which is further supported by neutron scattering findings.

SANS approach confirmed the credible micellar structure formation in 10%w/v normal and reverse BCPs and in their mixtures in varying % weight fraction with elevated temperatures in the aqueous homogeneous phase before the anomalous micellization occurs, i.e., cloudy zone (Figs. 4 and 5). Increased intensity in low Q region suggests the 2ϕ occurrences upon heating, whereas the presence of unimers or looping of unimers, i.e., Gaussian coil further leading to the clusters is witnessed in high Q region with poor scattering. Such substantial low Q scattering profile specifies the existence of large structures, i.e., clusters while the weak scattering in the mid-to-high Q range directs the interactions between BCP and solvent. Although the actual structure of "clusters" is unclear. However, reports on PEO and reverse Pluronic® 25R8 in D_2O provides understanding where PEO in D_2O create clusters as ethylene groups from different chains interact [21, 27, 31].

The fitted results for our examined single and mixed systems after employing various combinations of form factor and structure factor confirmed the micellar morphologies (Tables 1 and 2). The correlation length model was employed to fit the cluster and unimers. It was illustrated that 10%w/v L31 in low Q region remain as unimers with R_g ~ 8 Å at 20 °C and R_g ~ 8.2 Å at 25 °C (Table 1). Portion of the cluster reflect the high Q scattering. Such behavior attribute to the solvated PEO blocks getting stretched

Table 1 Fitted parameters from SANS analysis for 10%w/v normal and reverse BCPs in aqueous medium as a function of temperature

10%w/v BCP	T (°C)	a (Å)	b (Å)	Axial ratio	R_g (Å)	R_{hs} (Å)	N_{agg}	Micellar shape
L31	20	–	–	–	8.0	–	–	Unimers
	25	–	–	–	8.2	–	–	Unimers
31R1	15	–	–	–	13.4	–	–	Unimers
	19	–	–	–	14.7	–	–	Unimers
L64	30	37.4	37.4	1.0	9.1	49.9	65	Unimers + spherical
	37	35.6	35.6	1.0	–	55.7	76	Spherical
	50	63.7	33.1	1.9	–	–	101	Ellipsoidal
	60	325.7	35.3	9.2	–	–	588	Rod-like
17R4	30	–	–	–	14.4	–	–	Unimers
	37	–	–	–	16.6	–	–	Unimers
	38	–	–	–	18.0	–	–	Unimers
	39	–	–	–	18.4	–	–	Unimers
	40	–	–	–	18.4	–	–	Unimers
L35	30	–	–	–	10.0	–	–	Unimers
	37	–	–	–	10.7	–	–	Unimers
	50	24.3	24.3	1.0	8.8	82.3	39	Spherical
	60	26.7	26.7	1.0	18.2	82.3	52	Spherical
	70	31.0	31.0	1.0	23.6	142.5	81	Spherical
10R5	30	–	–	–	12.8	–	–	Unimers
	37	–	–	–	12.9	–	–	Unimers
	50	–	–	–	14.6	–	–	Unimers
	55	–	–	–	15.9	–	–	Unimers
P65	30	–	–	–	26.1	–	–	Unimers
	37	29.8	29.8	1.0	–	47.9	40	Spherical
	50	39.3	39.3	1.0	–	60.6	91	Spherical
	60	40.8	40.8	1.0	–	71.7	102	Spherical
25R4	30	–	–	–	14.3	–	–	Unimers
	37	–	–	–	18.1	–	–	Unimers
	38	–	–	–	18.5	–	–	Unimers
	39	–	–	–	19.0	–	–	Unimers
	40	–	–	–	19.0	–	–	Unimers

a, semi-major axis; b, semi-minor axis; R_g, radius of gyration of unimers; R_{hs}, hard sphere radius; N_{agg}, aggregation number

between PPO knots that scatter in a manner similar to free unimers in solution. Therefore, the scattering from the unimers and clusters cannot be distinctly differentiated. Likewise, 10%w/v 31R1 remain as unimers with $R_g \sim 13.4$ Å and ~ 14.7 Å at 15 °C and 19 °C and after that it show 2ϕ (Fig. 4). A 10%w/v mixture of L31:31R1 in varing ratio also remain as unimers. A 0.75:0.25 ratio shows the $R_g \sim 10.4$ Å at 25 °C, R_g for 0.50:0.50 ratio resides between the ~ 10.9 and ~ 11.7 Å at 15 °C and 25 °C respectively and for 0.25:0.75 ratio the R_g is ~ 15.5 Å at 25 °C (Fig. 5 and Table 2). Thus, greater R_g values with increasing ratio of BCP depicts L31 and 31R1 unimers are mixed properly and results into globular chain structure.

A 10%w/v L64 shows varied micellar transition from unimers to rod-like within the temperature scan examined. At 30 °C, there is a simultaneous presence of two geometries, i.e., unimers ($R_g \sim 9.1$ Å) and spherical micelles ($R_{hs} \sim 49.9$ Å and $N_{agg} \sim 65$). Also, spherical micelles are observed ($R_{hs} \sim 55.7$ Å and $N_{agg} \sim 76$) at 37 °C. These spherical micelles show micellar growth at 50 °C resulting in expanded ellipsoidal micelles ($a \sim 63.7$ Å, $b \sim 33.1$ Å, and $N_{agg} \sim 101$). Further aging the temperature up to 60 °C, these ellipsoidal micelles transform into rod-like micellar geometries ($a \sim 325.7$ Å, $b \sim 35.3$ Å, and $N_{agg} \sim 588$) progressively leading to 2ϕ around 62 °C. An increase in R_g from ~ 14.4 to ~ 8.4 Å with increasing temperature from 30 to 40 °C have been observed in 10%w/v 17R4. After 40 °C, clusters are expected as 17R4 will experience 2ϕ (Figs. 4 and 5). These findings go well with the reported work [24]. A very interesting observation was depicted in the mixed

Table 2 Fitted parameters from SANS analysis for 10%w/v normal and reverse BCPs mixture in varying ratio in aqueous medium as a function of temperature

10%w/v BCP	Ratio	*T* (°C)	*a* (Å)	*b* (Å)	*Axial ratio*	R_g (Å)	R_{hs} (Å)	N_{agg}		Micellar shape
								Normal	Reverse	
L31: 31R1	0.75:0.25	25	–	–	–	10.4	–	–	–	Unimers
	0.5:0.5	15	–	–	–	10.9	–	–	–	Unimers
		25	–	–	–	11.7	–	–	–	Unimers
	0.25:0.75	25	–	–	–	15.5	–	–	–	Unimers
L64:17R4	0.75:0.25	37	37.2	37.2	1.0	24.5	55.0	74	26	Spherical
	0.5:0.5	30	37.2	37.2	1.0	–	51.0	190	209	Spherical
		37	37.2	37.2	1.0	–	56.6	74	81	Spherical
		50	R_{cr} = 29.9 Å, L > 350 Å					–	–	Rod-like
	0.25:0.75	37	38.7	38.7	1.0	16.1	74.1	81	283	Spherical
L35:10R5	0.75:0.25	37	–	–	–	11.1	–	–	–	Unimers
	0.5:0.5	30	–	–	–	11.1	–	–	–	Unimers
		37	–	–	–	12.4	–	–	–	Unimers
		50	–	–	–	15.3	–	–	–	Unimers
		60	32.1	32.1	1.0	–	–	90	88	Spherical
	0.25:0.75	37	–	–	–	13.2	–	–	–	Unimers
P65:25R4	0.75:0.25	37	32.9	32.9	1.0	13.8	51.5	53	16	Spherical
	0.5:0.5	30	–	–	–	18.2	–	–	–	Unimers
		37	32.3	32.3	1.0	9.6	53.4	50	53	Spherical
		50	35.4	35.4	1.0	–	49.4	66	70	Spherical
		60	R_{cr} = 31.4 Å, L > 350 Å					–	–	Rod-like
	0.25:0.75	37	32.1	32.1	1.0	9.5	50.4	48	142	Spherical

R_{cr} cross-sectional radius, L length of rod-like micelle

BCP systems. The mixture of L64:17R4 demonstrated the spherical or ellipsoidal geometries (Table 2). A 0.75:0.25 ratio inferred the presence of spherical micelles at 37 °C with R_g ~ 24.5 Å and R_{hs} ~ 55.0 Å and N_{agg} ~ 74 (for L64) and 26 (for 17R4) which depicts more contribution of L64 than 17R4. For 0.50:0.50 ratio, it remains as spherical at 30 °C and 37 °C with R_{hs} ~ 51.0 Å and N_{agg} ~ 190 (for L64) and 209 (for 17R4) and R_{hs} ~ 56.6 Å and N_{agg} ~ 74 (for L64) and 81 (for 17R4) respectively while at 50 °C. It shows micellar transition from spherical to rod-like with R_{cr} ~ 29.9 Å and L ~ 350.0 Å (Fig. 5). Similarly, a 0.25:0.75 ratio exhibits the spherical micelle at 37 °C with R_g ~ 16.1 Å and R_{hs} ~ 74.1 Å and N_{agg} ~ 81 (for L64) and 283 (for 17R4). Here, the concentration of 17R4 in N_{agg} is higher in the mixed micelle.

A 10%w/v L35 due to equal EO/PO ratio, it was unable to make micelles at elevated temperature but micelle formation occurs at higher temperature. At 30 °C and 37 °C, L35 remains as unimers with R_g ~ 10.0 Å and 10.7 Å respectively. As temperature rises to 50 to 70 °C, the spherical micellar formed with R_{hs} ~ 82.3 Å and N_{agg} ~ 39 to R_{hs} ~ 142.5 Å and N_{agg} ~ 81 respectively. The cluster sizes are beyond the range of the SANS analysis. For 10%w/v 10R5, it also remains as unimers from 30 to 55 °C with R_g ~ 12.8 Å to ~ 15.9 Å (Fig. 4). Looking to the mixture of 10%w/v L35:10R5 in varing ratio, 0.75:0.25 remains as unimers at 37 °C with R_g ~ 11.1 Å while 0.50:0.50 ratio scrutinized as unimers with R_g ~ 11.1 ~ 15.3 Å from 30 to 50 °C but shows spherical micelles at 60 °C with R_{hs} ~ 32.1 Å and N_{agg} ~ 90 (L35) and 88 (10R5) due to equal contribution of L35 and 10R5. While for 0.25:0.75 ratio, it remains as unimers with R_g ~ 13.2 Å because both the BCP couldn't be able to form micelles at 37 °C (Fig. 5).

Unimers to ellipsoidal micellar transition observed from 30 to 70 °C for 10%w/v P65. P65 having equally hydrophilicity and hydrophobicity and similarly behave just like L35, it remains as unimers at 30 °C with R_g ~ 26.1 Å which tuned to spherical micelles at 37 °C with R_{hs} ~ 47.9 Å and N_{agg} ~ 40. These spherical micelles expanded its radius with temperature increased at 50 °C, i.e., R_{hs} ~ 39.3 Å and N_{agg} ~ 91. Further heating the solution, the micellar conversation was observed the spherical micelles were present at 60 °C with R_{hs} ~ 40.8 Å and N_{agg} ~ 102. At 10%w/v 25R4 with temperature range 30 to 40 °C, it exists as globular unimers with R_g of ~ 14.3 to ~ 19.0 Å (Figs. 4 and 5). As the temperature increases, large clusters appear. We put forward that the clusters get form as the insoluble PPO segment orient together to avoid the D_2O solvent interactions while the PEO segment still continue to remain hydrate in the solvent [13–15]. A 10%w/v P65:25R4 ratio demonstrates the spherical micelles for 0.75:0.25 ratio with R_{hs} ~ 51.5 Å and N_{agg} ~ 53 (P65) and 16 (25R4) at 37 °C. For 0.5:0.5 ratio, it remains as unimers at 30 °C

with R_g ~ 18.2 Å due to equal impact of 25R4, shows micellar transition into spherical with R_g ~ 9.6 Å and R_{hs} ~ 53.4 Å with N_{agg} ~ 50 (P65) and 53 (25R4) at 37 °C, R_{hs} ~ 49.4 Å and N_{agg} ~ 66 (P65) and 70 (25R4) at 50 °C. Interestingly, this mixed system shows rod-like micelle with R_{cr} ~ 31.4 Å and L ~ > 350 Å at 60 °C. A 0.25:0.75 ratio display the spherical geometry at 37 °C with R_g ~ 9.5 Å and R_{hs} ~ 50.4 Å and N_{agg} ~ 48 (P65) and ~ 142 (25R4) (Fig. 5). Here, the contribution of 25R4 is more due to its higher concentration. As the temperature rises, the scattering intensities rise, indicating an increase in the number of unimers or micelles. As a result, the peak shift towards high Q region reflecting the development of more micelles and a decrease in the intermicellar distance.

R_{cr}, cross-sectional radius; L, length of rod-like micelle.

As a conclusion form, Figs. 4 and 5 and Tables 1 and 2 demonstrate that the 10% w/v normal BCPs shows the micellar transitions from unimers to spherical to ellipsoidal to rod-like micelles as a function of temperature while 10%w/v reverse BCPs generally remains as unimers as a function of temperature which can be conclude that these are unable to make micelles as PPO remains at the end shows the less interaction and solubility in water. R_g results from the Guinier-Porod model appear consistent. These are apparent R_g because the fitting models do not consider the interparticle interactions. Also, the R_g is too small which is the SANS instrument detection limit, and so their size 10–20 Å is mentioned. This micellar transition shows the proper mixing of normal BCPs with reverse BCPs with was further depicted for the drug solubilization study. Results from scattering techniques have been reveal the mixed micellar geometries considering the low Q scattering profile and form factor whereas in high Q scattering profile, the structure factor dimensionality of the scattered particle is estimated from the calculated slopes proposed by Debye.

Drug solubilization prototype

Specific modern pharmaceutical formulations are very much imperative nowadays. An enormous amount of drug delivery schemes has been expansively established in last few ages. Hence, the understanding of drug solubilization in terms of dosage form is of extreme significance. Literature studies have reported the dynamic role of hydrophobic and electrostatic interactions governing the self-assembly in BCP micellar system that results into the varied aggregation in the presence of drugs to explore the solubilization agenda in aqueous solution [29–37]. However, the drug solubilization efficacies into the copolymers depend on the affinity between the drug and micellar shape of polymers. Thus, making an importance for such solubilization application, our study implies the solubilization study of the poorly water soluble anticancer drug, i.e., curcumin (Cur) in 10%w/v pure and mixed copolymeric solution employing spectral approach where a significant change in absorbance was measured.

It was noted that Cur remains highly soluble in 10%w/v normal polymeric solution due to spherical micellar geometries present while poorly soluble in the 10% w/v reverse polymeric solution due to the existence of unimers (Fig. 6). However, with addition of normal polymer in varying % weight fraction, the measured absorbance increases which endorses by the π to π^* transition which markedly increase the color intensity of Cur dissolved in varying ratio of reverse and normal copolymers, i.e., from light yellow to dark yellow (insight vial image in Fig. 6 a–c). Such behavior infers that the drug solubilization increases linearly as the micellization facilitate the probable morphology transition in micelles from unimers to spherical micelles as depicted from previous findings.

Briefly, the solubilization study was not performed for L31:31R1 due to lower CP values, i.e., it gets turbid at 30 °C. In L64:17R4 ratio, the solution remains lightest yellow in 10% w/v 17R4, also absorbance curve is slightly increased as compared to Cur dissolved in water due to presence of 17R4 unimers. As the varying proportion of L64 increase, the curve intensity increases with increase in yellow color intensity as shown in photograph (Fig. 6a). The quantitative amount of dissolved Cur in L64:17R4 are as following ~ 117.0 µM > ~ 106.7 µM > ~ 92.4 µM > ~ 3.7 µM > ~ 2.4 µM with varying ratios with 1:0, 0.75:0.25, 0.5:0.5, 0.25:0.75, 0:1 respectively (pink bar in Fig. 6d). The absorbance gets maximum and dissolved amount in case of 10%w/v L64 (1:0) is higher due to spherical micellar formation at 30 °C entrapped the Cur into the micellar core. In case of 0.75:0.25 ratio, also the dissolved Cur is higher due to higher influence of L64 on 17R4 while due to equal contribution in 0.5:0.5 ratio, the efficiency of Cur dissolution is bit lower. For 0.25:0.75 and 0:1 ratio, the 17R4 unimers are present more as compared to L64 that depicted 17R4 unimers are unable to solubilize Cur.

In case of 10%w/v L35:10R5 ratio, the absorbance curve intensity is smaller due to presence of unimers for all ratio of L35:10R5 at 30 °C which was unable to entrapped Cur, lightest color intensity observed due to less interaction between L35 and 10R5 unimers with Cur resulting into poor solubilization (Fig. 6b). The quantity of Cur in L35:10R5 ratios are resided between ~ 4.9 and ~ 1.5 µM for all ratio (blue bar in Fig. 6d).

For P65:25R4 ratio, the amount dissolved was little higher for 10% w/v 25R4 as compared to other reverse BCPs. After addition of P65, the curve peak increases and color intensity gets little intense due to more solubilization of Cur into P65 micelle (Fig. 6c). The soluble amount of Cur in 1:0 ratio is ~ 103.8 µM, in 0.75:0.25 ratio is ~ 100.7 µM, in 0.5:0.5 ratio is ~ 91.4 µM, in 0.25:0.75 ratio is ~ 42.2 µM and in 0:1 ratio is ~ 4.7 µM (gray bar in Fig. 5d). The higher amount of

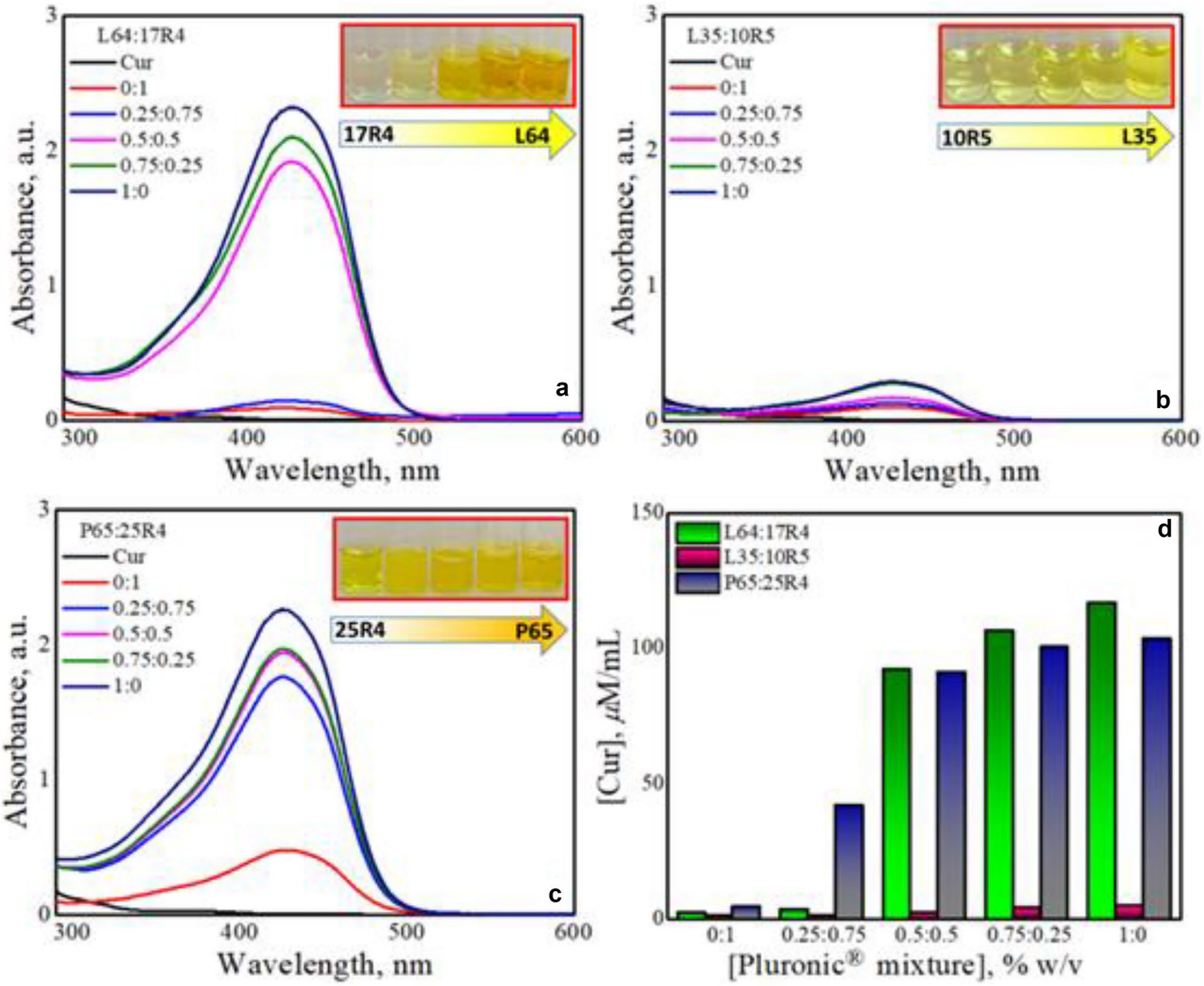

Fig. 6 Cur solubilization in single and mixture of 10%w/v normal: reverse BCPs in varying % weight fraction expressed qualitatively for **a** L64:17R4, **b** L35:10R5, **c** P65:25R4 revealing the change in the intensity (insight images of vials infer the physical appearance of the solution); and **d** quantitative scrutiny

Cur solubilization is due to P65 micelles formation, whereas 25R4 remains as unimers which unable to impregnate the Cur. Addition of 25R4 influences on the decrease solubility of Cur due to higher unimers geometry present.

In vitro *cytotoxicity*

Poor solubility and bioavailability are major concern in the therapeutic use of hydrophobic, water-insoluble drugs. Cur used in our study has poor bioavailability issues and require suitable cargos to overcome these hurdles without compromising its activity [38–42]. The prospective of Cur to provoke apoptosis in a variety of tumor tissues is well documented in the literatures [43–47]. Prevention against any disruption to the cell morphology (fibroblasts) by the Pluronic® mixture performance in absence and presence of Cur is put forth by cytotoxicity method using MTT assay (Figs. 7 and 8). To analyze the cytotoxicity of the examined compounds, we performed MTT assay in HeLa cells. Furthermore, we have seen the effect of compounds on cell morphology. The cells were treated with test compounds at 1 ng/mL and incubated at 37 °C for 1 h. They were fixed using 4% PFA and mounted using Mowiol. The control used was untreated cells. The cells treated with B4 and B10 compound show change in cell morphology (Fig. 7).

Insufficient water solubility and subsequent precipitation reduced the effective exposure period of free Cur-treated cells, resulting in lower cytotoxicity than Cur-loaded micelles (B1 in Fig. 7). Up to 60%, cells were viable at 200 ng/mL of Cur loaded Pluronics® micelles (Fig. 8).

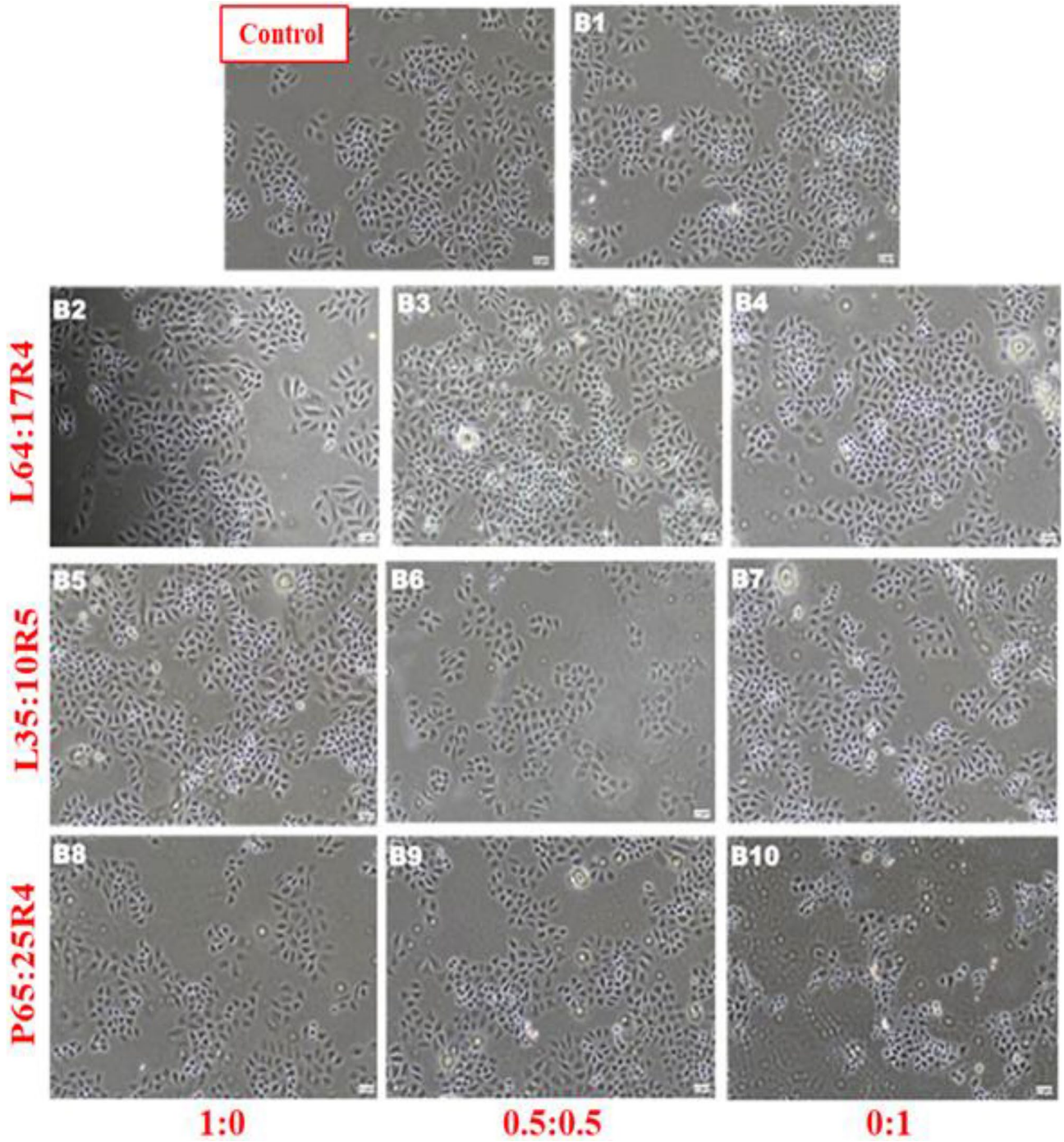

Fig. 7 Bright-field microscopic images of experimented HeLa cells

Furthermore, low cell viability of cancer cells, i.e., enhanced cytotoxicity was attributed as the dosage increased which infer the favorable solubilization of Cur in Pluronics® micelles. IC_{50} is the concentration value of the compound at which it kills 50% of the cells. We found that compounds B4 and B10 have IC_{50} values of 451.3 ng/mL and 310.3 ng/mL respectively. The other compounds (B1–B3, B5–B9) did have toxic effect but not enough to kill 50% of the cells. It may be as the Cur is encapsulated inside the polymer and polymer itself is non-toxic to the cells (Fig. 8).

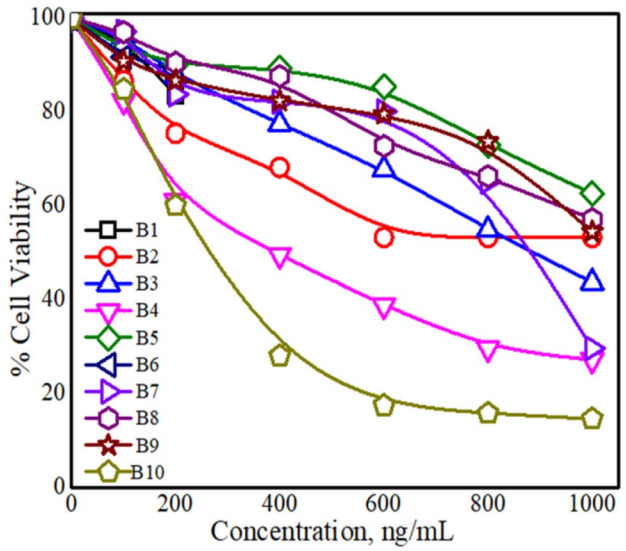

Fig. 8 Concentration-cell viability (dose–response) profile of HeLa cell exposed to Cur loaded polymeric mixture for 4 h

Conclusion

This work offers an insight into the phase behavior and self-assembly of normal and reverse BCPs in single and mix aqueous environment as a function of temperature. A comprehensive account on the clouding behavior of normal and reverse BCPs in varying %weight fractions demonstrated the influence of PPO on the CP, i.e., higher the PPO content, lower is the CP and vice versa. At elevated temperature, the CP decreases with the addition of reverse BCPs in mixed composition with normal BCPs. Thus, the temperature dependent unimers to micelle to 2ϕ obeyed the above rationale at practicable concentration in mixture. Using the scattering data obtained for varied range of BCP concentration and temperature, various geometries like unimers to spherical to ellipsoidal to rod-like micelles were inferred for normal BCPs. Despite their different structures, reverse BCPs share two corresponding morphologies: unimers (free polymer chains) and random network aggregates (clusters of > 1000 nm). By a judicious choice of the normal to reverse BCP ratio and giving an account to the formation of different morphologies of mixed micelles, the templates were used in the solubilization of anticancer drug (Cur) in normal and reverse BCP mixtures with the in vitro study using HeLa cells that exhibited good cytotoxicity. Thus, this study directs for experimental proven potential of Pluronic® mixtures on cancerous cell viability, thereby offering better prospects in designing chemically stable nanoscale objects for their possible applications in pharmaceutics.

Acknowledgements Authors acknowledge Department of Chemistry, Sardar Vallabhbhai National Institute of Technology (SVNIT), Gujarat-INDIA for providing the instrumentation facility.

Author contribution Dhruvi Patel: experimental investigation, methodology, data fitting and analysis, writing and editing. Payal Vaswani and Dhiraj Bhatia: biological activity and analysis, writing—review and editing. Debes Ray, Sumana Sengupta, Sharmishtha Dutta Choudhury and Vinod K Aswal: formal analysis, data fitting, writing—review and editing. Ketan Kuperkar: conceptualization, methodology, writing—review and editing, supervision, project administration. Pratap Bahadur: conceptualization, writing—review and editing, supervision.

Declarations

Conflict of interest The authors declare no competing interests.

References

1. Kuperkar K, Tiwari S, Bahadur P (2020) Self-assembled block copolymer nanoaggregates for drug delivery applications. Applications of polymers in drug delivery, Second Edition Elsevier, 15, 423–447, eBook ISBN: 978–0–12–819659–5
2. Li X, Park E, Hyun K (2018) Rheological analysis of core-stabilized Pluronic F127 by semi-interpenetrating network (SIPN) in aqueous solution. J Rheol 62:107–120
3. Rahdar A, Kazemi S, Askari F (2018) Pluronic as nano-carier platform for drug delivery systems. Nanomed Res J 3:174–179
4. Zarrintaj P, Ahmadi Z, Saeb M, Mozafari M (2018) Poloxamer-based stimuli-responsive biomaterials Mater Today: Proceedings 5:15516–15523
5. Kabanova A, Batrakova E, Alakhov V (2002) Pluronic® block copolymers as novel polymer therapeutics for drug and gene delivery. J Control Release 82:189–212
6. Patel D, Patel D, Ray D, Kuperkar K, Aswal V, Bahadur P (2021) Single and mixed Pluronics micelles with solubilized hydrophobic additives: underscoring the aqueous solution demeanor and micellar transition. J Mol Liq 343:117625–117635
7. Pitto-Barry A, Barry N (2014) Pluronic® block-copolymers in medicine: from chemical and biological versatility to rationalization and clinical advances. Polym Chem 5:3291–3297
8. D'Errico G, Paduano L, Ortona O, Mangiapia G, Coppola L, Celso F (2011) Temperature and concentration effects on supramolecular aggregation and phase behavior for poly(propylene oxide)-b-poly(ethylene oxide)-b-poly(propylene oxide) copolymers of different concentration in aqueous mixtures. J Coll Interf Sci 359:179–188
9. Akash M, Rehman K, Chen S (2014) Pluronic F127-based thermosensitive gels for delivery of therapeutic proteins and peptides. Polym Rev 54:573–597
10. Escobar-Chávez J, López-Cervantes M, Naïk A, Kalia Y, Quintanar-Guerrero D, Ganem-Quintanar A (2006) Applications of thermoreversible Pluronic F-127 gels in pharmaceutical formulations. J Pharm Pharm Sci 9:339–358
11. Jalaal M (2017) On the rheology of Pluronic F127 aqueous solutions. J Rheol 61:139–146
12. Guragain S, Bastakoti B, Malgras V, Nakashima K, Yamauchi Y (2015) Multi-stimuli-responsive polymeric materials. Chem Eur J 21:13164–13174
13. Lin Y, Paschalis A (2000) Small-angle neutron scattering investigation of the temperature-dependent aggregation behavior of the block copolymer Pluronic L64 in aqueous solution. Langmuir 16:8555–8561

14. Hung-Wei T, Ya-Huei H, Jing-Han W, Li-Jen C (2008) Novel behavior of heat of micellization of Pluronics F68 and F88 in aqueous solutions. Langmuir 24:13858–13862
15. Gangul R, Aswal V, Hassan P, Gopalakrishnan I, Kulshreshtha S (2006) Effect of SDS on the self-assembly behavior of the PEO-PPO-PEO triblock copolymer $(EO)_{20}(PO)_{70}(EO)_{20}$. J Phys Chem B 110:9843–9849
16. Patel D, Jana R, Lin M, Kuperkar K, Seth D, Chen L, Bahadur P, (2021) Revisiting the salt-triggered self-assembly in very hydrophilic triblock copolymer Pluronic® F88 using multitechnique approach. Coll Polym Sci 229–243
17. Alvarez-Ramirez J, Fernández V, Macías E, Rharbi Y, Taboada P, Gámez-Corrales R, Puiga J, Soltero J (2009) Phase behavior of the Pluronic P103/water system in the dilute and semi-dilute regimes. J Coll Interf Sci 333:655–662
18. Basak R, Bandyopadhyay R (2013) Encapsulation of hydrophobic drugs in Pluronic F127 micelles: effects of drug hydrophobicity, solution temperature, and pH. Langmuir 29:4350–4356
19. Popovici C, Popa M, Sunel V, Atanase L, Ichim D (2022) Drug delivery systems based on Pluronic micelles with antimicrobial activity. Polymer 14:3007–3022
20. Mata J, Majhi P, Guo C, Liu H, Bahadur P (2005) Concentration, temperature, and salt-induced micellization of a triblock copolymer Pluronic L64 in aqueous media. J Coll Interf Sci 292:548–556
21. Henda M, Gharbi A (2017) Temperature, concentration and salt effect on F68 tri-block copolymer in aqueous solution: Rheological Study. Polym Sci 59:445–450
22. Anderson B, Cox S, Ambardekar A, Mallapragada S (2002) The effect of salts on the micellization temperature of aqueous poly(ethylene oxide)-b-poly(propylene oxide)- b-poly(ethylene oxide) solutions and the dissolution rate and water diffusion coefficient in their corresponding gels. J Pharm Sci 91:180–188
23. Patel V, Ray D, Bahadur A, Ma J, Aswal V, Bahadur P (2018) Pluronic®-bile salt mixed micelles. Coll Surf B 166:119–126
24. Pérez-Sánchez G, Vicente F, Schaeffer N, Cardoso I, Ventura S, Jorge M, Coutinho J (2019) Rationalizing the phase behavior of triblock copolymers through experiments and molecular simulations. J Phys Chem C 123:21224–21236
25. Kumi B, Hammouda B, Greer S (2014) Self-assembly of the triblock copolymer 17R4 poly(propylene oxide)$_{14}$ -poly(ethylene oxide)$_{24}$-poly(propylene oxide)$_{14}$ in D_2O. J Coll Interf Sci 434:201–207
26. Chowdhry B, Snowdena M, Leharne S (1999) Scanning calorimetric investigations of phase transitions in a PPO-PEO-PPO block copolymer. Eur Polym J 35:273–278
27. Guiraud S, Alimi-Guez D, Wittenberghe L, Scherman D, Kichler A (2011) The reverse block copolymer Pluronic 25R2 promotes DNA transfection of skeletal muscle. Macromol Biosci 11:590–594
28. Dutra L, Ribeiro M, Cavalcante I, Brito D, Semião L, Silva R, Fechine P, Yeates S, Ricardo N (2015) Binary mixture micellar systems of F127and P123 for griseofulvin solubilization. Polímeros 25:433–439
29. El-Dahmy R, Elsayed I, Elshafeey A, Gawad N, El-Gazayerly O (2014) Optimization of long circulating mixed polymeric micelles containing vinpocetine using simple lattice mixture design, in-vitro and in vivo characterization. International J Pharmaceutics 477:39–46
30. Zhao L, Du J, Duan Y, Zang Y, Zhang H, Yang C, Cao F, Zhai G (2012) Curcumin loaded mixed micelles composed of Pluronic P123 and F68: preparation, optimization and in-vitro characterization. Coll Surf B 97:101–108
31. Lage E, Pillai S, Pal H, Bahadur A, Casas M, Sández-Macho I, Bahadur P (2018) Urea induced changes in self-assembly and aggregate microstructures of amphiphilic star block copolymers with widely different hydrophobicity. Coll Surf A 537:259–267
32. Patel D, Ray D, Kuperkar K, Pal H, Aswal V, Bahadur P (2020) Solubilization, micellar transition and biocidal assay of loaded antioxidants in Tetronic® 1304 Micelles. Polym Int 69:1097–1104
33. Patel D, Ray D, Kuperkar K, Aswal V, Bahadur P (2020) Parabens induced spherical micelle to polymersome transition in thermo-responsive amphiphilic linear and star-shaped EO-PO block copolymers. J Mol Liq 316:113897–113908
34. Patel D, Agarwal S, Ray D, Kuperkar K, Aswal V, Bahadur P (2021) An expedient in to the phase behaviour and scattering profile in PEO-PPO-PEO block copolymer mixed systems in aqueous solution. Coll Surf A 617:126330–126340
35. Zhang W, Shi Y, Chen Y, Ye J, Sha X, Fang X (2011) Multifunctional Pluronic P123/F127 mixed polymeric micelles loaded with paclitaxel for the treatment of multidrug resistant tumors. Biomaterials 32:2894–2906
36. Naskar B, Ghosh S, Moulik S (2012) Solution behavior of normal and reverse triblock copolymers (Pluronic L44 and 10R5) individually and in binary mixture. Langmuir 28:7134–7146
37. Hassanzadeh S, Feng Z, Pettersson T, Hakkarainen M (2015) A proof-of-concept for folate-conjugated and quercetin-anchored Pluronic mixed micelles as molecularly modulated polymeric carriers for doxorubicin. Polymer 74:193–204
38. Patel D, Rathod S, Tiwari S, Ray D, Kuperkar K, Aswal V, Bahadur P (2020) Self-Association in EO-BO-EO triblock copolymers as a nanocarrier template for sustainable release of anticancer drugs. J Phys Chem B 124:11750–11761
39. Iurciuc-Tincu C, Cretan M, Purcar V, Popa M, Daraba O, Atanase L, Ochiuz L (2020) Drug delivery system based on pH-sensitive biocompatible poly(2-vinyl pyridine)-b-poly(ethylene oxide) nanomicelles loaded with curcumin and 5-fluorouracil. Polymers 12:1450–1469
40. Song J, Liu Y, Guo Y, Zhong W, Guo Y, Guo L (2022) Nano–liposomes double loaded with curcumin and tetrandrine: preparation, characterization, hepatotoxicity and anti–tumor effects. Int J Mol Sci 23:6858–6871
41. Iurciuc C, Atanase L, Jérôme C, Sol V, Martin P, Popa M, Ochiuz L (2021) Polysaccharides-based complex particles' protective role on the stability and bioactivity of immobilized curcumin. Int J Mol Sci 22:3075–3099
42. Wu J, Qi C, Wang H, Wang Q, SunJ DJ, Yu G, Gao Z, Zhang B, Tian G (2022) Curcumin and berberine coloaded liposomes for antihepatocellular carcinoma therapy by blocking the cross-talk between hepatic stellate cells and tumor cells. Front Pharmacol 13:961788
43. Yadav V, Suresh S, Devi K, Yadav S (2009) Effect of cyclodextrin complexation of curcumin on its solubility and antiangiogenic and anti-inflammatory activity in rat colitis model. AAPS Pharm Sci Tech 10:752–762
44. Patel D, Kuperkar K, Bahadur P (2022) Temperature stimulated self-association and micellar transition for star shaped normal and reverse EO-PO block copolymers and their mixed systems as potential use for anticancer drug solubilization. Soft Matter 18:4543–4553
45. Kanoje B, Patel D, Kumar V, Sahoo S, Parikh J, Kuperkar K, (2019) Unraveling the solubilization and cytotoxicity study of poorly water-soluble anti-inflammatory drug in aqueous Gemini surfactants solution with physicochemical characterization and simulation study. Colloid Surf B, 179, 437–444
46. Braunová A, Chytil P, Laga R, Šírová M, Machová D, Parnica J, Říhová B, Janoušková O, Etrych T (2020) Polymer nanomedicines based on micelle-forming amphiphilic or water soluble polymer-doxorubicin conjugates: comparative study of in-vitro and in-vivo properties related to the polymer carrier structure, composition, and hydrodynamic properties. J Controlled Release 321:718–733
47. Shen T, Xu X, Guo L, Tang H, Diao T, Gan Z, Zhang G, Yu Q (2017) Efficient tumor accumulation, penetration and tumor

growth inhibition achieved by polymer therapeutics: the effect of polymer architectures. Biomacromol 18:217–230